J. Fluid Mech. (1986), *vol.* 173, *pp.* 225–251
Printed in Great Britain

Experimental and numerical study of vortex couples in two-dimensional flows

By Y. COUDER

Groupe de Physique des Solides, Ecole Normale Supérieure, 24, rue Lhomond, 75231 Paris Cedex 05, France

AND C. BASDEVANT

Laboratoire de Météorologie Dynamique, Ecole Normale Supérieure, 24, rue Lhomond, 75231 Paris Cedex 05, France

(Received 26 March 1986)

Two-dimensional turbulence is investigated experimentally in thin liquid films. This study shows the spontaneous formation of couples of opposite-sign vortices in von Kármán wakes. The structure of these couples, their behaviour and their role in turbulent flows is then studied using both a numerical simulation and laboratory results.

1. Introduction

In the last two decades, a number of theoretical, numerical and experimental studies have been devoted to the understanding of two-dimensional flow dynamics. These studies were mainly conducted by meteorologists for whom the two-dimensional dynamic is the fundamental model of large-scale atmospheric motion; for similar reasons oceanographers also worked on the subject. The first theories of two-dimensional turbulence were elaborated by Kraichnan (1967), Leith (1968) and Batchelor (1969). They are founded on a double-cascade concept: enstrophy (square of vorticity) is carried from injection scale to smaller and smaller scales until it reaches dissipation scales, while energy goes the other way, from injection scale towards ever larger scales. These theories, as well as the closure models which were developed afterwards (see Rose & Sulem 1978; Kraichnan & Montgomery 1980 for reviews) were mainly concerned with the spectral distribution of energy. Concurrently increasing computer power has led to accurate numerical simulation of two-dimensional flows, and, more specifically, of the enstrophy inertial range (Fornberg 1977; Basdevant *et al.* 1981; McWilliams 1984; Brachet 1986). However some of the numerical results suggest that the energy spectrum could significantly deviate from the law given by the phenomenological theory. Unfortunately atmospheric or oceanic measurements are not sufficiently reliable to settle the discussion (Babiano *et al.* 1985).

It is only recently that truly two-dimensional flows have been produced to a close approximation in laboratory experiments, and three different techniques have been developed. Three-dimensional motions are inhibited by a rotation (Hopfinger, Browand & Gagne 1982), or by Joule dissipation in mercury submitted to a strong magnetic field (Tsinober 1975; Sommeria 1983), or by steric constraint in the soap-film technique (Couder 1984). These laboratory experiments were able to give evidence of the reverse energy cascade predicted by the theory; however, the detailed study of the enstrophy cascade has not yet been achieved with laboratory apparatus.

One impact of these laboratory experiments has been to stimulate the studies, already begun with direct numerical models, of the spatial structures in two-dimensional turbulent flows. In several numerical simulations of well-developed turbulence there has been observed, amidst a rapidly evolving turbulent medium, the appearance of long-lived organized structures. Such structures appear in decaying turbulence as well as in forced steady flows. Amongst these structures were motionless isolated strong vortices and also fast translating couples of vortices of opposite signs that usually dissociated rapidly. McWilliams (1983) has shown that these structures resist the enstrophy cascade; Basdevant, Couder & Sadourny (1984) have also compared the vorticity dynamics to the passive-scalar dynamics and shown that a characteristic of vorticity is its tendency to concentrate in isolated structures. Interactions between isolated vortices have been studied theoretically for a long time.

An isolated axisymmetric vortex is the simplest steady solution of high-Reynolds-number two-dimensional turbulence; however, an isolated vortex is motionless. To obtain a moving steady solution one must consider at least two vortices. Usually entities formed of two vortices are called pairs. However, their properties are very different according to whether the two vortices are of similar or opposite sign. For clarity in the present paper we shall call two interacting vortices of the same sign *a pair*, and two interacting vortices of opposite sign *a couple*. It is well known that two vortices of the same sign, if close enough, will interact irreversibly through the vortex-pairing process until they merge into a unique larger vortex. Conversely the existence, in two-dimensional flows, of stable, isolated couples of vortices of opposite sign with a fast translating motion was predicted in several theoretical works (Thomson 1867; Lamb 1916; Batchelor 1967; Deem & Zabusky 1978; Pierrehumbert 1980). The stability of some of these couples was demonstrated by the technique of contour dynamics (Deem & Zabusky 1978; Pierrehumbert 1980), the couples were then called V-states.

Similar phenomena have also been studied, theoretically or numerically, in a meteorological context and called modons (Stern 1975; Larichev & Reznik 1976; Flierl *et al.* 1980; McWilliams *et al.* 1981): in the β-plane approximation large-scale atmospheric motions are modelled by the two-dimensional Navier–Stokes equation together with a linear dispersive term representing the variation of Coriolis forces with latitude; these modons have been found to be soliton-like solutions of the equation. Interactions and collisions of modons have been studied numerically on the β-plane by McWilliams & Zabusky (1982) and McWilliams (1983).

We present here the results from a study of the role of structured vortex couples in two-dimensional turbulence. The particularity of our approach has been a constant interaction between laboratory experiments and numerical simulations. For this reason we shall try to give an integrated account of the results of both in order to show how they complement each other. In the first part of the article, we shall describe the experimental and numerical techniques that we used, giving particular attention to the difficulties inherent to each one and to the approximations that they imply. Unwanted effects can arise in both experiment and simulation but since they are very different in nature comparison between the two helps to rule out the possibility of experimental or numerical artefacts.

The results will be presented chronologically showing how they led us from experiment to simulation and back.† We shall first recall the initial experimental results which clearly show the spontaneous formation of structured couples in a turbulent wake. The decomposition of a wake into couples is also obtained experi-

† Part of these results were presented previously in Couder, Basdevant & Thomé (1984) and Basdevant *et al.* (1984).

mentally in a non-turbulent regime by a modulation of the velocity. Simulations confirm these results and permit precise measurements of the vorticity field of one of the resulting couples. These measurements show that the couple is a linear one of the type described by Lamb (1916) and Batchelor (1967). We shall then examine under which conditions couples of that type can form. Numerical simulation is well adapted to the systematic attempts implied, because it permits easily the defining of many different initial states. We shall conclude that a quadrupolar interaction helps to fasten the vortices together. Finally, if these couples are very active, owing to their fast translating motion, their lifetime is limited by collisions with other structures. We shall show experimentally and numerically how a gas of couples decays.

2. The experimental and numerical techniques

2.1. *Experimental technique*

Common observation of soap films shows that they appear fluid and that motion can easily be induced in their plane. It is very tempting to study two-dimensional flows in these films: owing to their extreme thinness two-dimensionality is easily maintained and the use of a suspended film avoids the effect of friction on the walls of a container.

However such films have not, until recently, been used in classical fluid-dynamics experiments. Most of the works devoted to soap films have been concerned with what makes them extraordinary objects: their very singular physico-chemical, thermodynamical and topological properties. Less interest has been given to their ordinary properties as a thin fluid layer.

The question to be answered here, to evaluate the value of using soap films, is whether or not their specific properties impose themselves so strongly as to hide the general characteristics of two-dimensional flows. In such a case the results of experiments in soap films would lose generality, and comparison with classical fluids would become impossible.

We shall only describe those aspects of the experimental apparatus concerning the precautions taken to make the soap film as normal a fluid as possible. As we are not studying specific properties of soap films the choice of the soap solution is dictated by practical concerns. The film has to be long lived and to be mobile (Mysels, Shinoda & Frankel 1959) with a low surface viscosity. Similar results can be obtained with many solutions of various soaps. As we required reproducible drainage behaviour and viscosity we always used identical solutions prepared a few hours before the experiments. All the experiments reported here were performed with a commercial soap composed of a mixture of sodium lauryl sulfate and sodium benzene sulfate. Experience shows that for very weak concentrations the films immediately after stretching are thick and drain fast while for stronger concentrations the films are much thinner and drain more slowly. An optimum between these opposite requirements is found for a 0.3 % solution of our soap. Addition of 10 % of glycerol increases the stability of the film.

We use large frames 65×24 cm made of threaded rods that we simply dip into the soap solution to stretch a film. The frame is then placed horizontally in the experimental set-up. Under its own weight the film becomes concave (upward). As the initial thickness is not homogeneous the thicker zones will move to the lower part of the film at its centre while the thinner zone will move up near the frame. When lit with monochromatic sodium light the film exhibits interference fringes which show the equal-thickness lines. They form concentric ellipses round the centre (figure 1*a*).

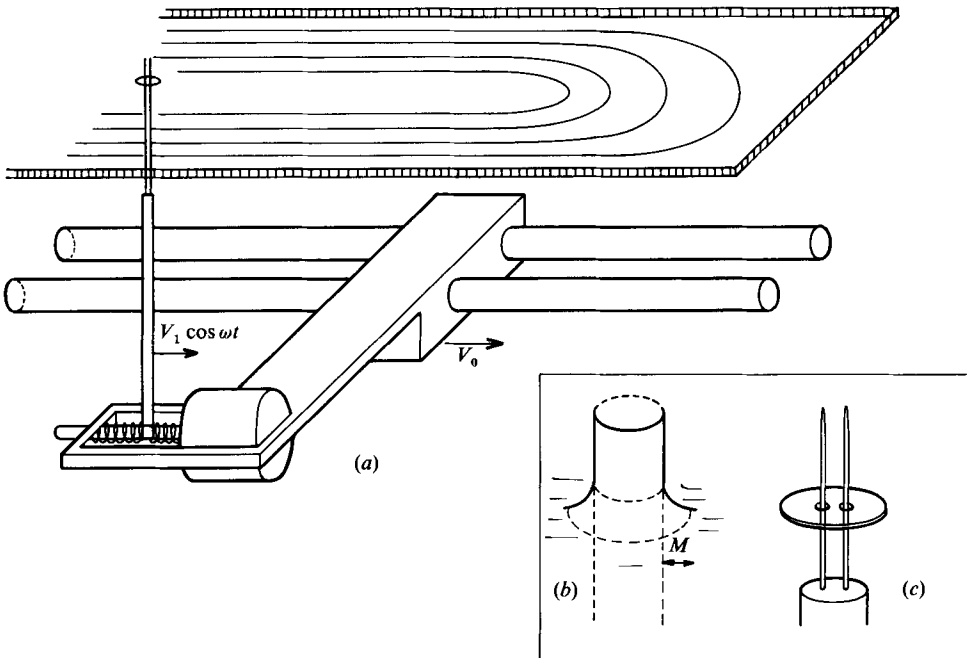

FIGURE 1. (*a*) Schematic drawing of the experimental set-up showing the moving carriage and the electromagnet which sets the cylinder in vibration. A slotted plate (not shown here) separates the moving carriage from the soap film so that global motions of the air do not disturb the film. (*b*) The cylinder and its meniscus. (*c*) The mounting of the aluminium paper disk.

The frame is slightly warped so that these ellipses are as elongated as possible. If the soap solution has been chosen adequately the interference fringes are, for several minutes, relatively far apart in the central regions but very close together near the border. In the central region of the film two difficulties are minimized. First, the film has a relatively large thickness e ($\approx 10\,\mu$m) so that it has sufficient inertia, and motion is not too rapidly damped by air friction. Secondly, it is horizontal and has a relatively constant thickness so that the effects of buoyancy in a stratified fluid are avoided.

It should be noted that the film is not in equilibrium and that while we work it drains constantly. The interstitial fluid tends to flow towards the centre. This flow is very slow in our films and can be neglected over the time of evolution of a wake. It only necessitates the frequent renewal of the film. In old films, drainage tends to increase the thickness gradients near the centre until a drop forms.

The present study relies experimentally on the visualization of the flows. We take photographs and videotape recordings of the evolution of the interference fringes of the film during its motion. In the central zone under study, the initial thickness of the film at rest is not strictly constant either after stretching because of the initial disorder, or later because of its draining. In both cases fringes are present before the experiment begins. Once the film is set into motion these fringes show patterns related to the structure of the flow. Two effects of different timescales contribute to this visualization.

On short timescales each element of the film as it moves retains its own thickness so that the slight initial variations of thickness are advected by the flow as if it were

a passive scalar. The resulting visualization is the same as that produced by an unevenly distributed colourant.

Thickness, however, is not a passive scalar. In that respect we can compare the soap films to the thin layers of fluid in shallow-water experiments. In these the fluid motion is not divergence-free as the fluid layer tends to thin down at the centre of the vortices. Furthermore surface waves can be generated and coupled to the motion.

In soap films however, because of the elastic properties of the surface, the situation is different. We are concerned with the symmetrical waves (Taylor 1959) that correspond to thickening or thinning of the film. Vrij *et al.* (1970) showed that surface elasticity in soap films damped them very strongly. In our experiment we only observed a slow thinning of the film at the centre of the vortices. As this divergent flow is opposed by the elasticity of the surfaces it only occurs through the motion of the interstitial fluid relative to the surfaces. As the film is very thin this viscous flow is very slow. It is only if the vortices are long lived that concentric fringes will show up in their central region.

We towed two types of obstacle to produce wakes in the film. The first was a cylinder, of diameter d, made of stainless steel, and so it has to be wet before being set through the film to prevent the bursting of the membrane. Two difficulties arise: firstly the cylinder is surrounded by a meniscus which is towed with it (figure 1*b*) so that the effective diameter of the obstacle becomes $d+2m$. The width m of the meniscus can only be deduced *a posteriori* from observation of the wake. The frequency f_{ST} of vortex emission can be measured on videotape recordings and compared with the predicted values of the Strouhal frequency. For velocities u_0 such that $Re \approx 150$ we can use the empirical relation found by Roshko (1954),

$$St = \frac{f_{ST}(d+2m)}{u_0} = 0.212 - \frac{4.5}{Re}.$$

We deduce $2m$ from f_{ST} and find values generally of the order of 0.1 cm, so that the correction to the diameter of the cylinders ($d \approx 0.2$, 0.3 or 0.4 cm) is important. Unfortunately since the shape of the meniscus in a film is not reproducible and more or less fluid can accumulate in it, $2m$ has to be determined for each experiment. The second problem is that the cylinder also creates a wake in the air. As the kinematic viscosity of air is several times larger than that of the film the Reynolds number and the characteristics of the wake in the air and the film are different; the disturbing role of the air motion, though weak, is difficult to evaluate.

For these reasons we have developed a second technique better adapted to the two-dimensionality of the film. The obstacle is now a very thin (20 μm) disk of aluminium paper of diameter d which floats in the film. As the thickness of the disk is of the same order of magnitude as that of the film, the bordering meniscus has a negligible size and the effective diameter of the obstacle is d. The problem of towing the disk is a little tricky as the film is not plane and the disk has to remain in its surface. We first used a thin needle passing through a large hole in the disk. Surface tension maintains the disk in the film and it moves up and down the needle. However, this was not entirely adequate as the disk was also free to oscillate in rotation under the influence of vortex emission. As we wanted our results to be comparable to the classical experiments in bulk fluids where the cylinder is fixed we finally used the system shown on figure 1 (*c*). The disk is free to move up and down two thin parallel needles so that oscillation is blocked. The wake of the needles in air is negligible, the

observed motion is localized in the film and simply damped by the motionless air that surrounds it.†

The cylinder or needles are mounted on a carriage which moves (figure 1*a*) on two cylindrical rails. Velocities up to 100 cm/s can be reached. It can also be set in vibration either longitudinally or transversally at frequencies $5 < f_m < 200$ Hz (see details on figure 1*a*).

2.2. *The numerical model*

The numerical model integrates in time the two-dimensional Navier–Stokes equation

$$\frac{\partial \omega}{\partial t} + \boldsymbol{V} \cdot \operatorname{grad} \omega = F(\omega) + D(\omega),$$

where $\omega = \operatorname{curl} \boldsymbol{V}$ is the (scalar) vorticity of the flow, and F and D respectively represent forcing and dissipation terms. The flow is supposed to be periodic on a square of side $L = 10$ cm; this hypothesis, which may at first sight look unrealistic, is in fact not restrictive provided the size of the flow structures is much smaller than the period L. Periodicity, which permits avoiding spurious vorticity generation by boundary effects, is mainly chosen to take advantage of the power of the Fourier-spectral techniques for spatial discretization. The model uses a 128×128 regular collocation grid in physical space. Partial derivatives with respect to space coordinates are evaluated at collocation points by means of spectral decomposition in Fourier space; in wavenumber space we use a circular truncation at $K_* = 60.8$ (i.e. waves with wavelength shorter than L/K_* are suppressed).

With respect to time discretization, the time scheme is second-order centred (leapfrog) for nonlinear terms and exact integration for linear dissipative terms. Experiments discussed here concern freely decaying turbulence (no forcing, $F = 0$).

The numerical technique has several limitations, the first of which is its limited resolution. To avoid pathological effects due to truncation we use for the dissipation D a super-dissipation operator, instead of the classical Laplacian operator (which either would be ineffective if used with the true kinematic viscosity, or would impose an excessively low Reynolds number)

$$D(\omega) = -\frac{1}{\tau}(\lambda_* \mathrm{D})^8(\omega)$$

where $\lambda_* = L/2\pi K_*$ is the cutoff scale and τ is a characteristic timescale of the subgrid-scale parameterization (Basdevant & Sadourny 1983). Let us briefly recall that the goal of this parameterization technique is to concentrate the dissipation effects in small scales, thus maximizing the ratio of dissipated enstrophy to dissipated energy in accordance with two-dimensional turbulence theory. Being built with partial-derivative operators, the super-dissipation also preserves spatial structures of the flow. The numerical code, together with this parameterization technique, has previously been extensively used in the study of homogeneous two-dimensional turbulence (Basdevant *et al.* 1981). The drawback of virtual-scale parameterization

† Situations where a flat obstacle creates a quasi-two-dimensional wake in its plane exist in nature. Satellite photographs show the atmospheric flow to the leeward of isolated oceanic islands such as Madeira (Chopra & Hubert 1964; Zimmerman 1969). The stratocumulus clouds have large-scale eddy patterns forming a von Kármán wake which only appears when the meteorological situation is such that a regular wind blows and that a temperature inversion blocks the vertical exchanges. The periodicity of the wake is related to the diameter of the island $d \approx 80$ km (while its mean altitude is only ≈ 1 km). In certain photographs isolated couples of vortices are possibly observed far downstream.

is that the Reynolds number of the flow is no longer well defined: it can only be estimated through inspection of the scale of the smallest dynamically active structures. Another limitation of our numerical technique is that it cannot simulate the proper boundary conditions of the laboratory experiment and their consequences: the shedding of vortices behind a moving cylinder. The initial alternate collection of vortices of a von Kármán street has thus to be given as initial state or obtained through the destabilization of a double velocity shear.

Finally one also has to be careful, when examining the results of a numerical experiment, to verify whether the flow is influenced by the internal symmetries of the method and of the grid; in most experiments, random noise must be included in the initial state in order to break the grid symmetries.

The numerical model was run on an array processor AP120, and the typical computing time for a numerical experiment was about a hundred times that for a similar laboratory experiment! (1000 s/10 s).

3. Experimental and numerical results on the formation of vortex couples in wakes

3.1. *Experiment: spontaneous emergence of couples in turbulent wakes*

When cylinders of various sizes are towed in a fluid the threshold velocity for a vortex wake to be formed is inversely proportional to the cylinder diameter d. However this is not observed in thin soap films: the same velocity is necessary to reach the threshold with $d = 6$ mm and $d = 4$ mm. The reason is that with a large disk and a small velocity the vortex turnover time is large. The characteristic timescale imposed on film motions by air damping then hinders the formation of the vortices. We shall thus limit ourselves to obstacles with $d = 0.2$ and 0.3 cm for which the threshold of appearance of vortices in thick films can be considered to correspond to the classical Reynolds-number criterion.

In films of thickness $e \approx 10$ μm we found an effective viscosity $\mu_F \approx 3 \times 10^{-2}$ Poise, which is the sum of the bulk viscosity of the interstitial water and of the surface viscosity of the two superficial layers

$$\mu_F = \mu_b + \frac{2\mu_S^s}{e};$$

so $\mu_S^s = 10^{-5}$ surface Poise.

Standard von Kármán wakes can be observed in the range $50 < Re < 150$. For larger values of Re the wake is no longer stable. The first two-dimensional destabilization occurs longitudinally when some vortices are advected by the mean flow at the centre of the wake. Usually two vortices destabilize simultaneously, are sucked in by the preceding ones, and merge with them (figure 2). The phenomenon can be almost periodic so that, for instance, two out of four or two out of five vortices, etc. will be absorbed. For values $Re > 150$ a secondary wake with a longer wavelength can form. In our film damping is too strong to permit judgement but we doubt that this secondary wake could be stable. This merging of vortices in wakes was previously observed by Taneda (1959) in bulk fluids. Therefore in these fluids they precede the three-dimensional destabilization.†

For larger values of the Reynolds number a cascade of such pairings occurs leading to ever larger vortices. The wake has the characteristic behaviour of two-dimensional turbulence with energy cascading towards larger structures and stretched zones of

† Two-dimensional stability of von Kármán wakes has been theoretically investigated by Saffman & Schatzman (1982) and Meiron, Saffman & Schatzman (1984).

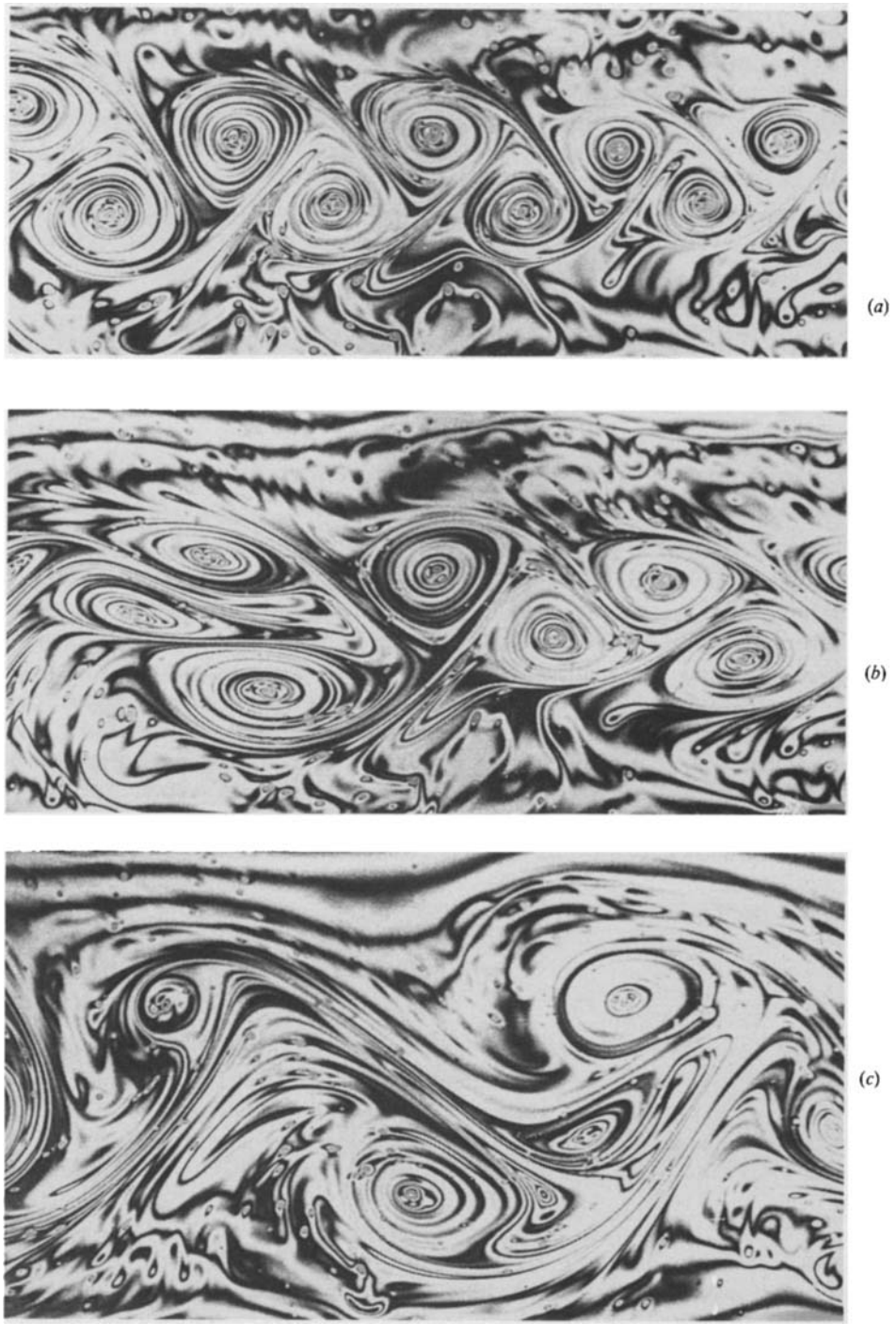

FIGURE 2. Three successive (in time) photographs showing vortices merging in a turbulent wake.

FIGURE 3. Vortex couples formed in a turbulent wake.

weak vorticity dissipating slowly. The width of the wake in this regime increases slowly at the same rate at which the vortices grow in size through successive merging processes.

For $Re > 400$ a new phenomenon occurs. Couples of vortices of opposite sign escape rapidly out of the wake. The faster couples (figure 3) have a circular envelope. A couple moves under its own velocity field; if the two vortices are of equal intensity it has a rectilinear fast translating motion, if they are unequal the trajectory is concave on the side of the stronger vortex and it moves in an arc of a circle.

This behaviour corresponds to a previous observation by Aref & Siggia (1981) who showed in a numerical simulation the possibility of the escape of couples in the destabilization of a double row of vortices.

The wake then has a very different aspect; the central part, very similar to that described previously, is dominated by pairing and merging processes but on each side the escaping couples form an expanding cloud. Most of the couples moving in circles of various radii will return to the central zone and be destroyed there. The faster translating ones can move very far away until they are dissipated by viscosity. In our experiment however they are stopped by the stratification effect in the inclined bordering zones of the film.

Any vibration of the cylinder has a strong influence. It considerably increases the number of couples that may form for a given value of Re and it decreases the threshold Re at which couples appear. This property is not limited to the turbulent regime and will be discussed in §3.3.

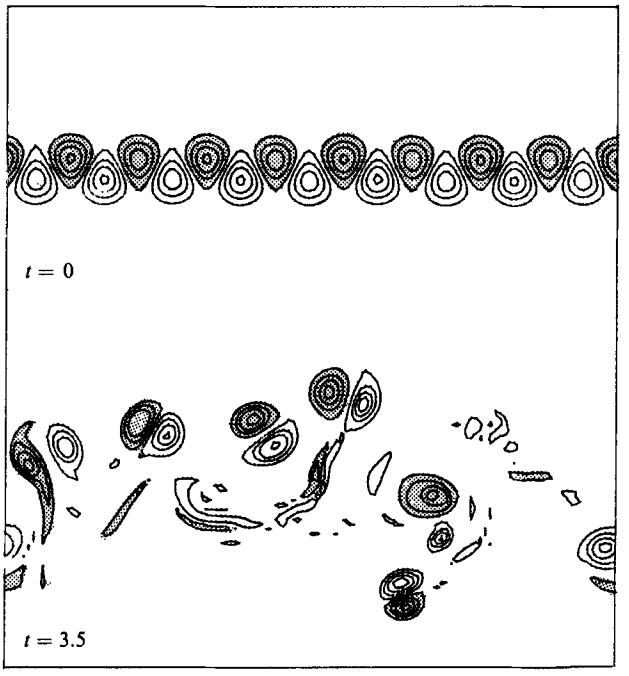

FIGURE 4. The computed evolution of a double row of vortices showing isolines of vorticity at times $t = 0$ and 3.5. The positive vortices (shaded) are initially above the wake axis, so that the whole wake moves towards the right.

3.2. *Numerical simulation of the turbulent wakes*

It is not possible with the spectral code to introduce solid boundary conditions and so the phenomena that occur behind the disk cannot be reproduced. We can obtain reasonably realistic evolutions of turbulent von Kármán streets in two ways.

An artificial von Kármán street can be imposed as an initial condition using the well-known geometrical characteristics of the position of the vortices. The initial state is built with $2n$ alternate vortices, each with a Gaussian stream function.

It is also possible to simulate the evolution of an initial double shear with a velocity profile similar to those observed in the near wake of a flat plate. Its destabilization shows the formation of a von Kármán street and its subsequent evolution.

Both simulations give similar results in good qualitative agreement with the experiment. The first destabilization of a turbulent wake occurs through merging processes, the second through formation of vortex-couples. Figure 4 shows the evolution of an artificial wake and the resulting cloud of couples that surrounds it.

As in the experiment the addition of a spatial modulation to the initial state increases the number of couples created.

3.3. *The effects of a modulation on the evolution of the wake and the creation of couples*

The large effect of all modulations of the velocity on the density of created couples in a turbulent wake was an incentive to investigate the effect of a controlled modulation on non-turbulent wakes. The issue is complicated by the fact that two different effects can result from a modulation. One is linked with the destabilization

of a modulated double row of vortices, the other is due to changes in the regimes of shedding of vorticity behind the cylinder. We shall discuss these effects separately as the first is best observed numerically and the second experimentally.

3.3.1. *Destabilization of the von Kármán wake*

If, in a nearly regular double row of vortices, two opposite vortices get nearer to each other and further from their other neighbours their interaction will tend to make these two vortices move away together. Furthermore we shall show in §4.2 that the influence of the other neighbours tends to compass them into a tightly linked couple. Careful observation of the destabilization of turbulent wakes obtained in both experiment and simulation shows that this is indeed the main process by which couples are formed in the turbulent wakes. Here, uneven spacing and strength of the vortices corresponds to the appearance of randomness with a large range of spatial and temporal frequencies. It could be foreseen that modulating the vortex position or strength at a controlled spatial frequency would lead to systematic formation of couples when the frequency is chosen to be related to the spatial periodicity of the wake. Practically this can be done in a numerical simulation by introducing a spatial modulation of the width of a double shear in the initial condition. Regimes with periodic formation of couples are then observed (J. M. Chomaz private communication, 1985). These results are interesting by themselves as they show that induced modes of two-dimensional destabilization of a double row of vortices can lead to systematic formation of couples. However, as we shall see, they are not directly comparable with the experimental situation.

3.3.2. *Change in the vortex-shedding regime*

Experimentally it is not possible to impose directly a spatial modulation to the wake. The only possibility is to modulate the velocity of the fluid relative to the cylinder.

The effects of such modulation have already been investigated. Griffin & Ramberg (1976) studied the effect of longitudinal vibrations of the cylinder at frequencies larger than the Strouhal frequency f_{ST}. Their photographs show that couples tend to form at certain frequencies. Since they worked with bulk fluids three-dimensionalization of the flow hinders further development of the two-dimensional effects. Recently E. Detemple & H. Ecklemann (private communication, 1986) obtained a similar modulation by superimposing on a flow of gas a sound wave of large amplitude.†

In our experiment the disk is now vibrating in direction of u_0 so that its velocity is

$$u = u_0 + u_1 \cos(2\pi f_m t).$$

Both the amplitude u_1 and the frequency f_m are tunable. We explored the effects of modulation frequencies $0.5 f_{ST} < f_m < 2.0 f_{ST}$. For a small amplitude of modulation the vortices are still emitted at the usual Strouhal frequency. The effect of the modulation is to make the wake less regular and, as discussed previously, it leads to couple formation in the turbulent case. For $Re < 200$ however air damping weakens the vortices too rapidly and their evolution cannot be observed for long enough to observe induced periodic formation of couples.

† With smoke visualization and anemometry their technique allowed Detemple & Eckelman to perform a precise analysis of the flow as a function of the modulation frequency. They find, for large sound amplitude, modulated wakes very similar to ours.

When the amplitude u_1 is large enough ($u_1 > 0.15\ u_0$) the modulation frequency imposes itself and governs the shedding of vorticity behind the disk. The systematic study of the resulting effects would go beyond the scope of the present article but we shall describe here the changes observed in the conformation of the wake as they involve the creation of couples.

In the natural shedding behind a non-vibrating disk two vortices of opposite sign are present behind the disk and they detach alternately on each side every half Strouhal period. In the forced wakes a modulation of period $T_m = 1/f_m$ causes two vortices of opposite sign to detach almost simultaneously at each period T_m when the velocity of the disk is maximum, $u_0 + u_1$. We shall now describe the resulting wakes for various frequencies f_m.

(i) $f_m \approx f_{ST}$. When the modulation frequency is very close to the Strouhal frequency the forced wake resembles the natural one (figures 5*a*, *b*) except that vortices of opposite sign are brought closer together two by two. The couples thus formed translate with a velocity $u_c = \beta u_0$ at an angle θ with the direction of u_0. As they all move in the same direction the wake drifts sideways and is no longer symmetrical with respect to the axis defined by the direction of u_0.

(ii) $0.5 f_{ST} < f_m < f_{ST}$ and $f_{ST} < f_m < 1.5 f_{ST}$. The wake has similar characteristics both below and above the Strouhal frequency. As shown in figures 5 (*c*, *d*) it is formed of couples shed at each period of the modulation. Successive couples have their velocity directed alternately on each side of the wake. For this reason the apparent periodicity of the wake formed of staggered couples is twice the distance separating two successively emitted couples.

Figure 6 shows how series of frames from videotape recordings are interpreted. At time 0 the disk is at A and a couple is emitted. At time Δt this vortex couple has moved to B ($AB = u_c\,\Delta t$) in a direction θ with the axis while the disk has moved to C ($AC = u_0\,\Delta t$). A picture taken at time Δt shows the disk at C and the vortex couples emitted during the interval Δt at B, B', B'' etc. They are staggered on two symmetrical straight lines at angles γ with the axis of the wake (figure 6), γ is entirely defined by the values of u_0/u_c and θ:

$$tg\gamma = \frac{\sin\theta}{\frac{u_0}{u_c} - \cos\theta}.$$

Successive couples are emitted at A and A' at a distance $AA' = u_0 T_m$, T_m being the modulation period. The apparent periodicity of the staggered wake as measured on the axis is

$$\lambda' = HH'' = (u_0 - u_c \cos\theta)\, 2T_m$$

and the distance $l' = BB''$ between two successive couples on the same side of the wake is

$$l' = BB'' = \frac{(u_0 - u_c \cos\theta)\, 2T_m}{\cos\gamma}.$$

This spatial periodicity can be compared with the periodicity of the natural von Kármán wake where the vortices all translate at a velocity $u_u = \alpha u_0 = 0.16\ u_0$ so that the vortices have a special periodicity $\lambda_{ST} = (u_0 - u_u)\, T_{ST} \approx 0.84\ u_0\, T_{ST}$.

Over the whole range $u_0 - u_c \cos\theta/\cos\gamma$ remains close to $u_0 - u_u$ so that the observed distances are always approximately such that

$$\frac{l'}{\lambda_{ST}} \approx 2\frac{T_m}{T_{ST}}.$$

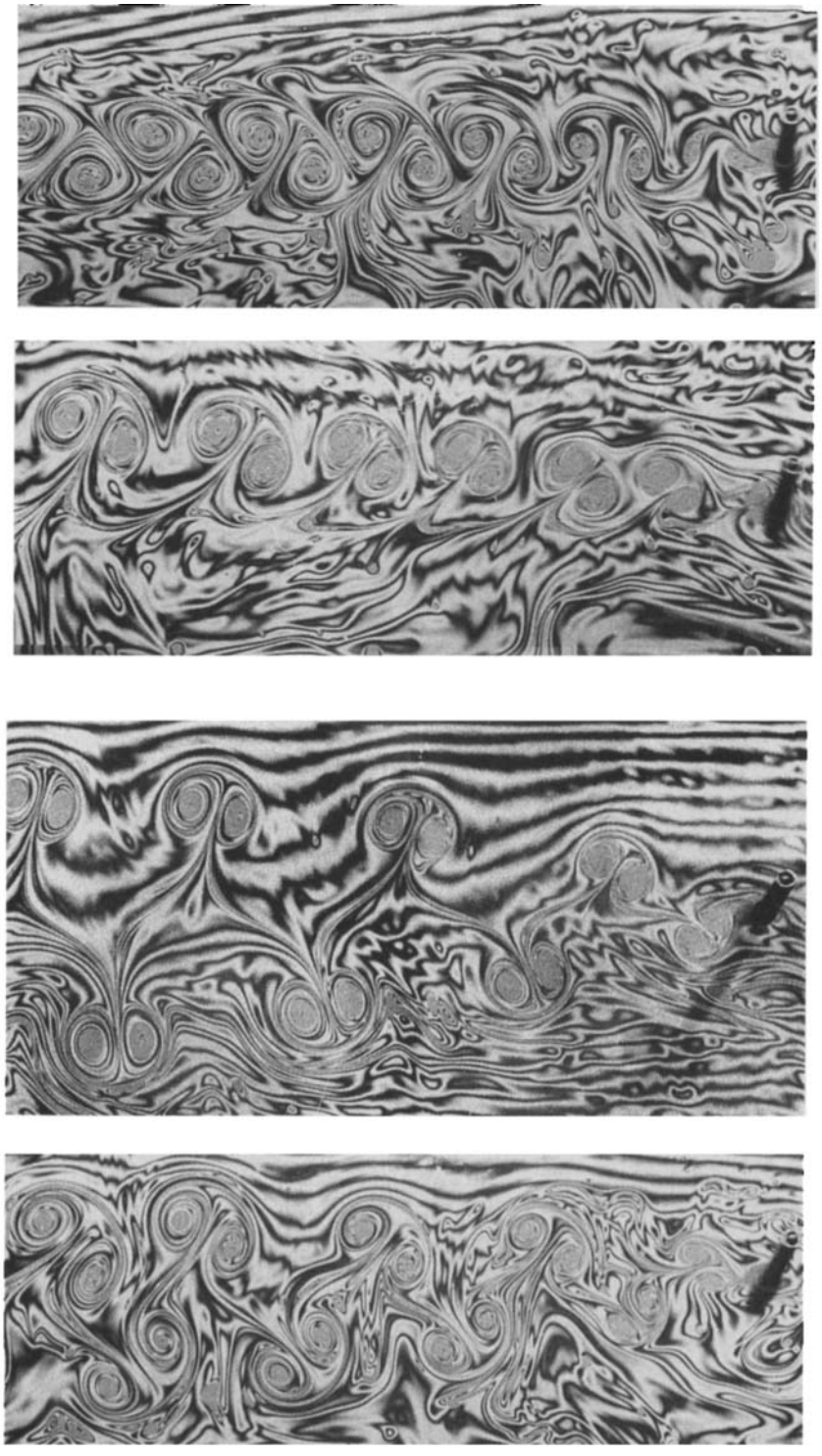

FIGURE 5 (*a–d*). For caption see page 238.

FIGURE 5. (*a*) The natural von Kármán wake of a cylinder of effective diameter $d+2m \approx 0.4$ cm towed at $u_0 = 21.5$ cm/s; $f_{ST} = 10$ Hz, $\lambda_{ST} = 1.75$ cm. (*b*) The forced wake of a cylinder oscillating in line at a frequency $f_m \approx f_{ST}$: $d+2m = 0.4$ cm, $u_0 = 45$ cm/s, $f_m = 22$ Hz, $f_{ST} = 21$ Hz, $\lambda_m = 1.8$ cm. (*c*) $f_m \approx 1.15 f_{ST}$. The wake is formed of isolated couples: $d+2m = 0.4$ cm, $u_0 = 29$ cm/s, $f_m = 15$ Hz, $f_{ST} = 13$ Hz, $\lambda' = 3.28$ cm. (*d*) $f_m \approx 1.4 f_{ST}$. The couples are less tightly formed and remain interacting. (*e*) $f_m \approx 1.7 f_{ST}$. Interaction between the couples shed successively leads to pairing and the wake becomes asymmetrical. (*f*) $f_m \approx 2 f_{ST}$. The shedding of large vortices is inhibited, small couples are shed symmetrically on the central zone of the wake remains as an unstable double shear. All these photographs have the same scale.

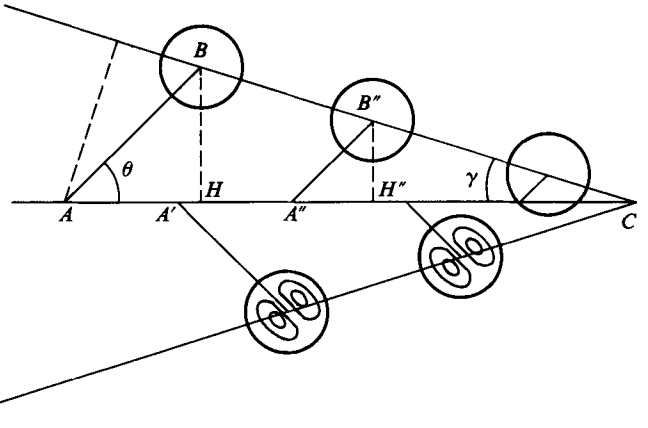

FIGURE 6. Sketch showing the characteristic angles and lengths of a wake formed of staggered couples.

FIGURE 7. The cloud of couples created in a turbulent wake with $f_m = 1.1 f_{ST}$.

But in the present range of frequencies the aspect of the wake changes as θ and u_c vary.

(iii) For the lower frequencies $f_m \approx 0.6 f_{ST}$ the vortices are shed less frequently so that larger vorticity is concentrated in them and they form fast translating couples $u_c \leqslant 0.35\, u_0$ emitted at small angle ($\theta \approx 20°$).

(iv) Near the Strouhal frequency the couples still move fast with larger θ ($\theta \approx 45°$) so that the angle γ is largest in this range ($\gamma \approx 15°$ on figure 5*c*).

(v) For values of $f_m \approx 1.4 f_{ST}$ the vortices become weaker, the couples are less tightly formed so that u_c becomes small ($u_c \approx 0.15\, u_0$). Furthermore the couples can no longer be considered as non-interacting. The resulting wake is a double row of couples with a small value of γ (figure 5*d*).

(vi) $f_m \approx 1.7 f_{ST}$. All the preceding analysis assumes that the couples are non-interacting and formed of opposite vortices of equal strength so that they move in a straight line. This is not always the case, in particular for $f_m \approx 1.7 f_{ST}$ when the couples as they detach are very close to each other immediately behind the cylinder. As shown on figure 5(*e*) the two vortices of positive sign of two successive couples are so near each other that they undergo pairing. The resulting positive vortex remains coupled to a negative vortex on one side of the wake while the other negative vortex remains isolated. Thus the wake becomes asymmetrical with a series of isolated vortices on one side and a series of unequal couples moving backward in an arc of a circle on the other side.

(vii) $f_m \approx 2 f_{ST}$. The emission of large vortices is inhibited by the vibration, small secondary couples are emitted symmetrically while the central part of the wake forms a double shear which will destabilize further downstream.

Finally we can compare natural and modulated wakes when they become turbulent. As we saw previously the first destabilization, in the non-modulated case, is due to

the pairing instability and corresponds to the inverse energy cascade building up larger structures in two-dimensional turbulence. For the same values of the Reynolds number a modulated wake of the staggered-couples type remains practically regular as the couples are too far away from each other to interact. For larger values of the Reynolds number ($Re \approx 400$) the shedding becomes less regular so that the couples start moving in random directions and form a cloud (figure 7). This type of turbulent motion is characterized by its expansion as couples invade surrounding quiescent zones. We shall see however (§4.3.2) that when the density of couples is large enough collisions tend to destroy them leading to a weak normal decaying two-dimensional turbulence.

4. Vortex couples

4.1. *Structure*

Although the soap-film experiment provides a good visualization of the flow and clearly shows the circular envelope of the vortex field, it is easier to analyse the detailed structure of a couple from numerical-experiment results. Figure 8(*a*) displays a vortex couple from a numerical simulation that had reached a stable shape and was free from any disturbances. On figure 8(*b*) vorticity profiles of this couple are compared with those of the theoretical model given in Batchelor (1967). This model corresponds to a steady solution of the two-dimensional Euler equation, for which the vorticity vanishes outside a circular envelope of radius a and is, inside, proportional to the relative stream function

$$\omega = \begin{cases} 0, & r > a, \\ \left(\dfrac{3.83}{a}\right)^2 \Psi_r, & r < a. \end{cases}$$

The relative stream function being

$$\Psi_r = \begin{cases} 0, & r > a, \\ -CJ_1\left(\dfrac{3.83r}{a}\right)\sin\theta, & r < a, \end{cases}$$

the uniform translation velocity of the structure is then

$$V = \tfrac{1}{2}C\,\frac{3.83}{a}\,J_0(3.83).$$

J_0 and J_1 are the first two Bessel functions.

The comparison on figure 8(*b*) of Batchelor's model with the observed couple is strikingly good; the small discrepancies with the theoretical model, such as the slight asymmetry between the front and back of the numerical couple may be explained by the influence of the rest of the fluid or by the fact that the couple is not completely steady. Figure 8(*c*) displays a scatter graph of the relative stream function Ψ_r versus the vorticity ω for the same experimental couple; on this figure the linear relation between stream function and vorticity inside the couple and the vanishing of vorticity outside appears clearly. This confirms that the fastest couples we observe, experimentally and numerically, are couples of the type described by Lamb and Batchelor, that we shall call hereafter linear couples.

We shall now explore the elementary processes by which two vortices of opposite sign may form such a linear couple.

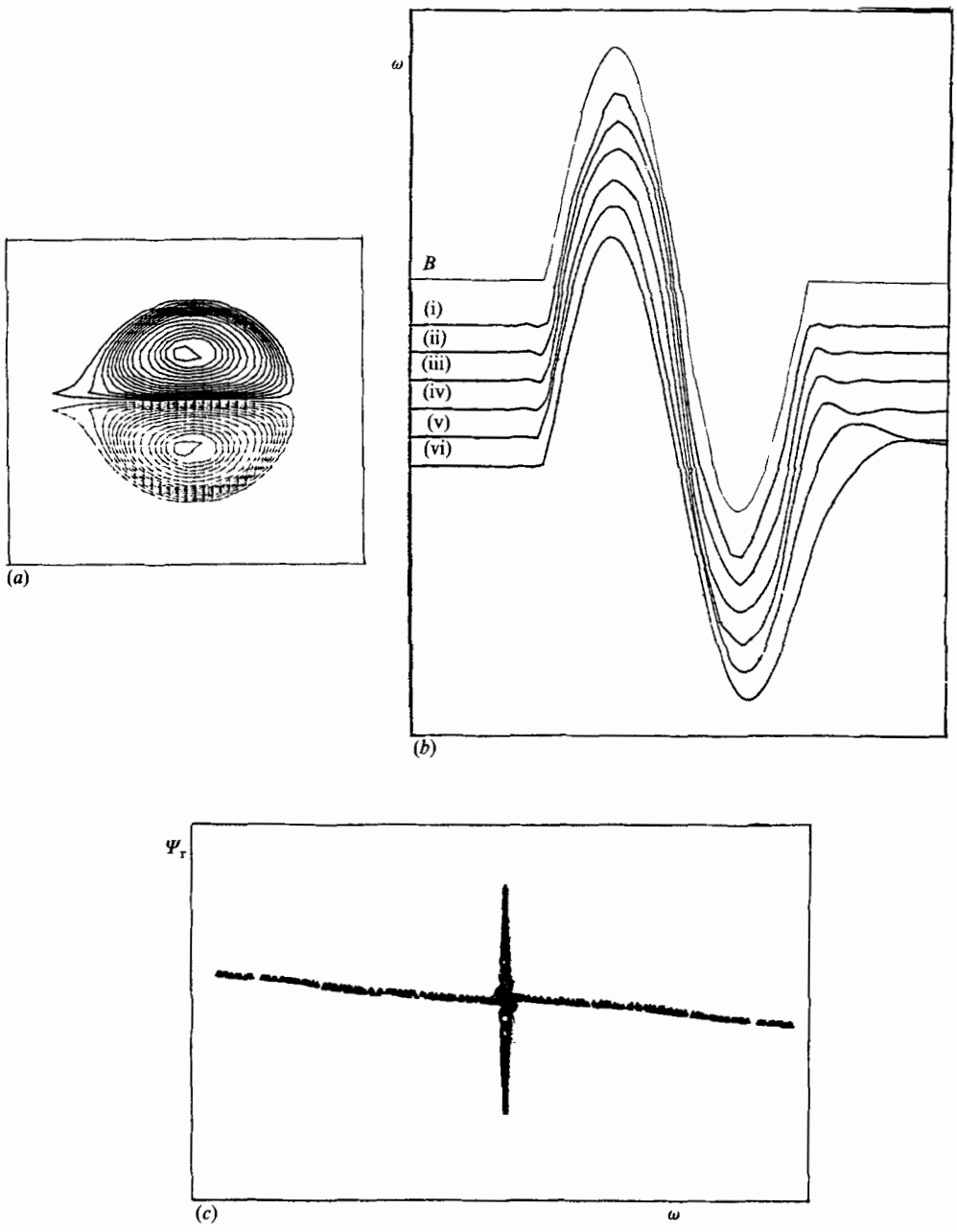

FIGURE 8. (*a*) Enlargement of a vortex couple obtained numerically (vorticity isolines). The positive vortex is above the symmetry axis; the couple moves towards the right. (*b*) Vorticity profiles across a couple, compared with the model given by Batchelor. Curve R displays the Batchelor's reference at $\theta = \frac{1}{2}\pi$. Curves (i)–(vi) display $\omega/\lambda \sin\theta$, where ω is the vorticity, θ the polar axis of the section, λ a correcting factor: (i) $\theta = \frac{1}{2}\pi$, $\lambda = 1$; (ii) $\theta = \frac{1}{3}\pi$, $\lambda = 1$; (iii) $\theta = \frac{1}{4}\pi$, $\lambda = 1.05$; (iv) $\theta = \frac{1}{6}\pi$, $\lambda = 1.23$; (v) $\sin\theta[0.2$, $\lambda = 1.49$; (vi) $\sin\theta = 0.1$, $\lambda = 1.52$. (*c*) Scatter plot of the relative stream function Ψ_r versus the vorticity ω for the couple displayed on (*a*).

4.2. *The formation of couples*

4.2.1. *Elementary processes*

Two vortices of opposite signs, if left initially sufficiently close to each other, will interact; they will undergo mainly a translation motion, each vortex being translated under the velocity field of the other. This is illustrated in an experiment (figure 9*a*) in which the vorticity field was initiated with two vortices of opposite signs, each with a Gaussian structure. Figure 9(*b*) shows the scatter graph of the relative stream function versus the vorticity of the couple after it had reached a steady shape. One may see on this figure that the two vortices had evolved towards a nonlinear couple, that is a steady solution of Navier–Stokes equations. Looking at the vorticity profile drawn on figure 9(*c*), one may notice another difference between this nonlinear couple and a linear couple: the slope breaking of the vorticity profile between the two vortices marks out the weaker linkage of the nonlinear couple.

Experimentally two vortices left alone will never evolve towards a linear couple. We found numerically that in order to obtain a linear couple initial conditions must be of quadrupolar type, so that a kind of compression effect forces the two vortices together. This is illustrated on figure 10 where the flow was initiated with two vortices of opposite signs but with Gaussian stream-function structure: each vortex is then surrounded with a 'coat' of opposite sign vorticity. In the subsequent evolution the role played by the coats is clearly seen: their effect is to initially slow down the two vortices by compressing them against each other.† A similar effect is obtained in the destabilization of an initial state where four alternate vortices of slightly unequal strength are initially lined up (figure 11).

Once the two vortices have been coupled they remain so and move faster. For identical strength of the vortices, and same initial separation, the velocity of the linear couple of figure 10 is four times the velocity of the nonlinear couple of figure 9 (this is best seen on the video film of our numerical results).

Another way of creating linear couples through quadrupolar interactions is to provoke a collision of two nonlinear couples. This can be seen on figures 12 and 13 where two nonlinear couples collide at an angle of 90°: two of the vortices are compressed into a linear couple easily recognizable by its characteristic circular shape. Figure 13 was obtained experimentally by the collision of two couples near a wake. Numerically we also obtained formation of couples from various quadrupolar initial states.

So far we have studied the coupling of two vortices of opposite sign but identical in other respects. When studying tentative coupling of asymmetric vortices we found that in order to obtain a couple the vortices must not differ too much in strength (total vorticity) and in extent (diameter) otherwise one vortex will be distorted strongly by the velocity shear induced by the other. Slightly asymmetric couples may be formed, their trajectory being curved toward the side of the stronger vortex. Asymmetry in extent tends to be reduced by the loss of vorticity filaments from the larger vortex.

4.2.2. *Formation in turbulent wakes*

Amongst turbulent fields the formation of vortex couples is particularly frequent in two-dimensional turbulent wakes. We can now explain why the von Kármán wakes form an initial state likely to promote their generation. All the vortices created behind

† This effect was first noticed by H. Fabre and B. Laviron (unpublished work).

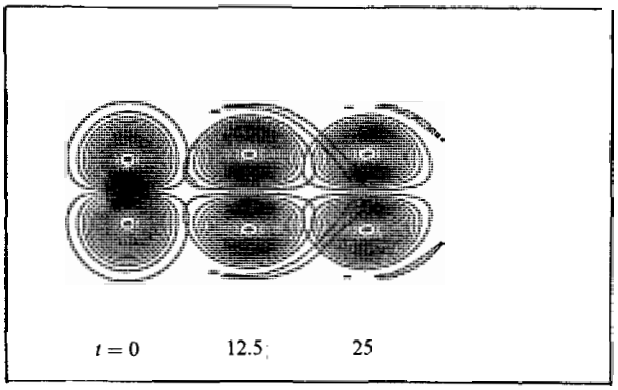

(*a*)

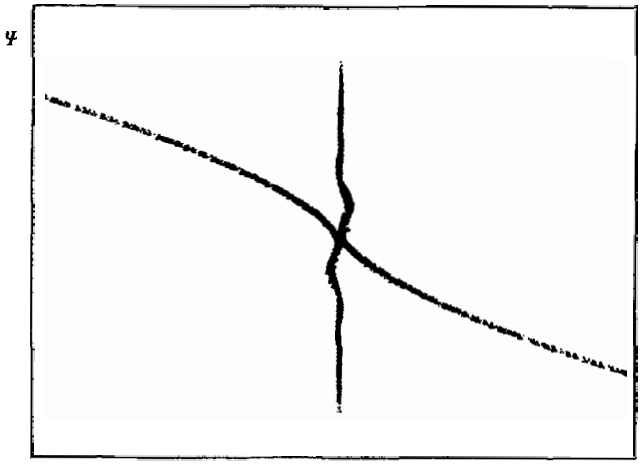

(*b*)

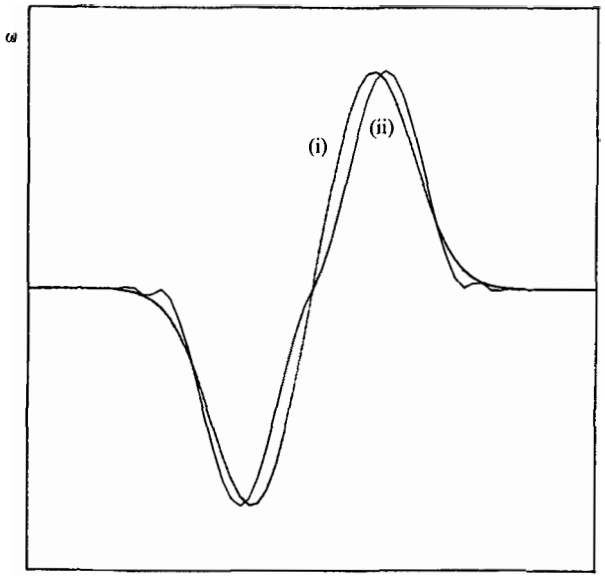

(*c*)

FIGURE 9. (*a*) Vorticity contours at times $t = 0$, 12.5 and 25 for an initial state of two vortices of opposite signs. The positive vortex is above the symmetry axis. (*b*) Scatter plot of the relative stream function Ψ_r versus the vorticity ω for the state $t = 25$ of (*a*). (*c*) Vorticity profile across the couple of (*a*). (i) $t = 0$; (ii) 25.

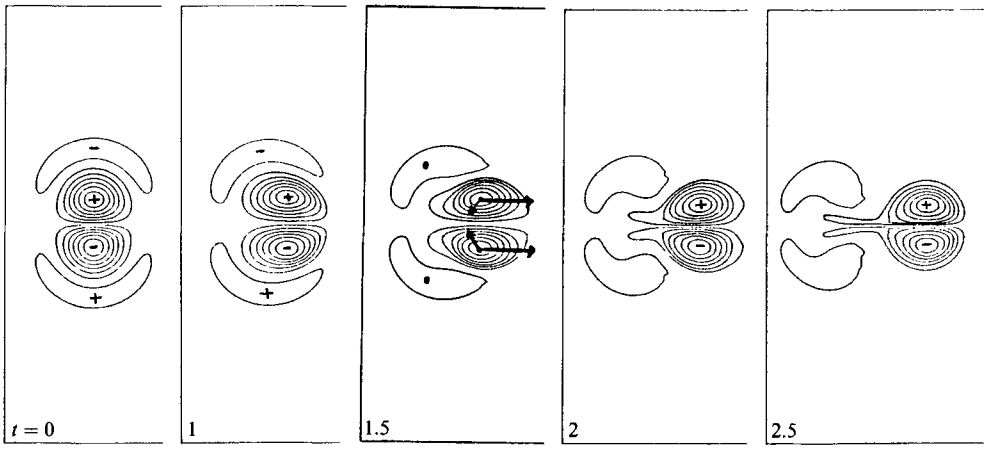

FIGURE 10. Couple initiated from two coated vortices: vorticity contours at times $t = 0$, 1, 1.5, 2 and 2.5. At time 1.5, to illustrate the compression effect, we draw arrows indicating the action on a vortex of the other vortex and of its own vorticity screen (as if they were point vortices).

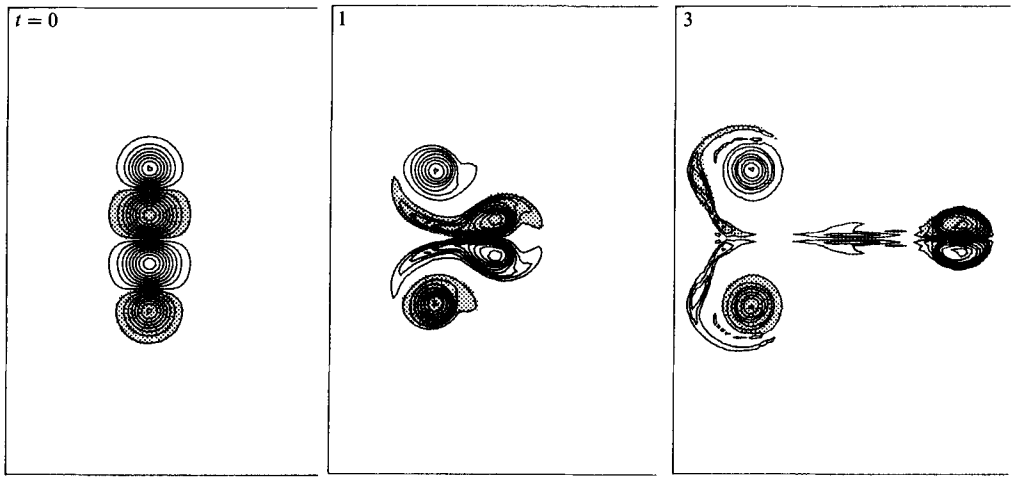

FIGURE 11. Couple initiated from four alternate vortices of nearly equal strength, regularly spaced in a row: Vorticity contours at times $t = 0$, 1 and 3.

the cylinder are of similar shape and strength and are alternate in sign. Slight modifications of the regular wake may lead to quadrupolar patterns suitable for the formation of a couple. If these modifications result from the irregularity in the turbulent regime the creation of couples happens randomly. A periodic modulation increasing the quadrupolar situation increases considerably the number of couples.

4.3. *The couples' future*

When vortex couples move across the fluid they encounter other couples, or isolated vortices, or weak remnants of vorticity. This leads to various types of collision or interaction. We shall first study numerically the possible elementary processes, then examine their effect statistically.

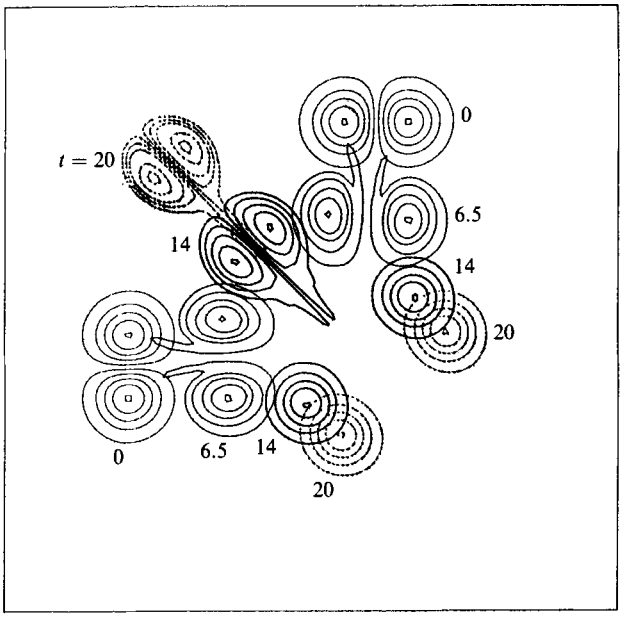

FIGURE 12. Collision of two nonlinear couples (initiated as in figure 9*a*). They collide at an angle of 90°. Vorticity contours at times $t = 0$, 6.5, 14 and 20 are superimposed on the same figure.

4.3.1. *Elementary processes*

Head-on collisions of two modons have been investigated by McWilliams & Zabusky (1982). They are elastic and lead, after exchange of partners, to the formation of two new couples moving at right angles to the original ones.

Other collisions can be characterized by the angle θ at which the trajectories of the couples' axes intersect. These collisions, to be elastic, must be symmetrical (at the time when the collision occurs the two couples must be located symmetrically with respect to the bisector of the angle θ). Non-symmetrical collisions are usually inelastic and may produce various results: coalescence of two vortices of the same sign or shearing of a vortex into two smaller ones (figure 14). If the angle of the trajectories is too small (of the order of less than 20°) there will be pairing and merging of the vortices of the same sign.

The interaction between a couple and an isolated vortex can also, depending upon the exact conditions, be either elastic with a change of partner, or inelastic. Finally the couples often move in a medium with a background of weak vorticity. McWilliams *et al.* (1981) have shown that a modon encountering structures with a few percent of its own strength may be disassociated.

A characteristic of the collision processes is their sensitivity to initial conditions: a very slight change in the position or the direction of the motion of a couple can change an elastic lateral collision into an inelastic destructive process. With interactions the positional unpredictability leads to unpredictability of the structures themselves. For this reason, only observation of the resulting statistical properties permits estimation of the role of the couples in various turbulent situations.

4.3.2. *Evolution in a turbulent field*

Wakes. In a turbulent wake where only a small number of couples is created the evolution of the central part of the wake remains dominated by merging processes

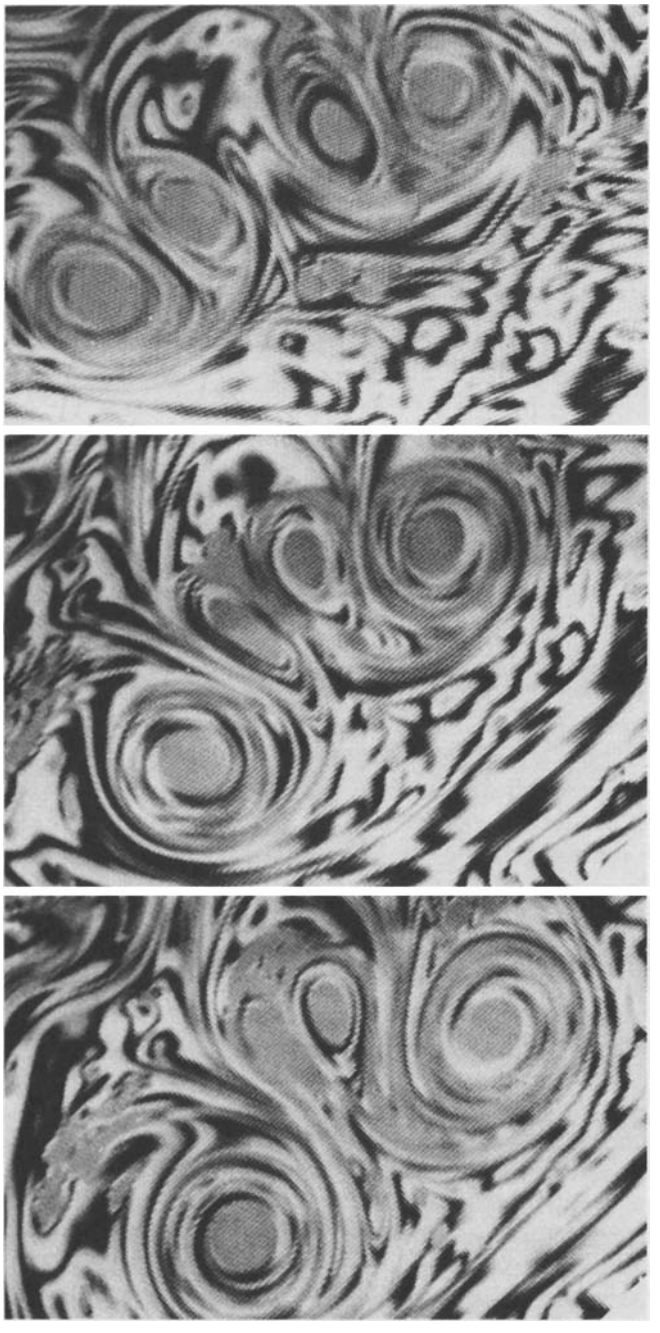

FIGURE 13. Experimental collision of vortex couples in a soap film.

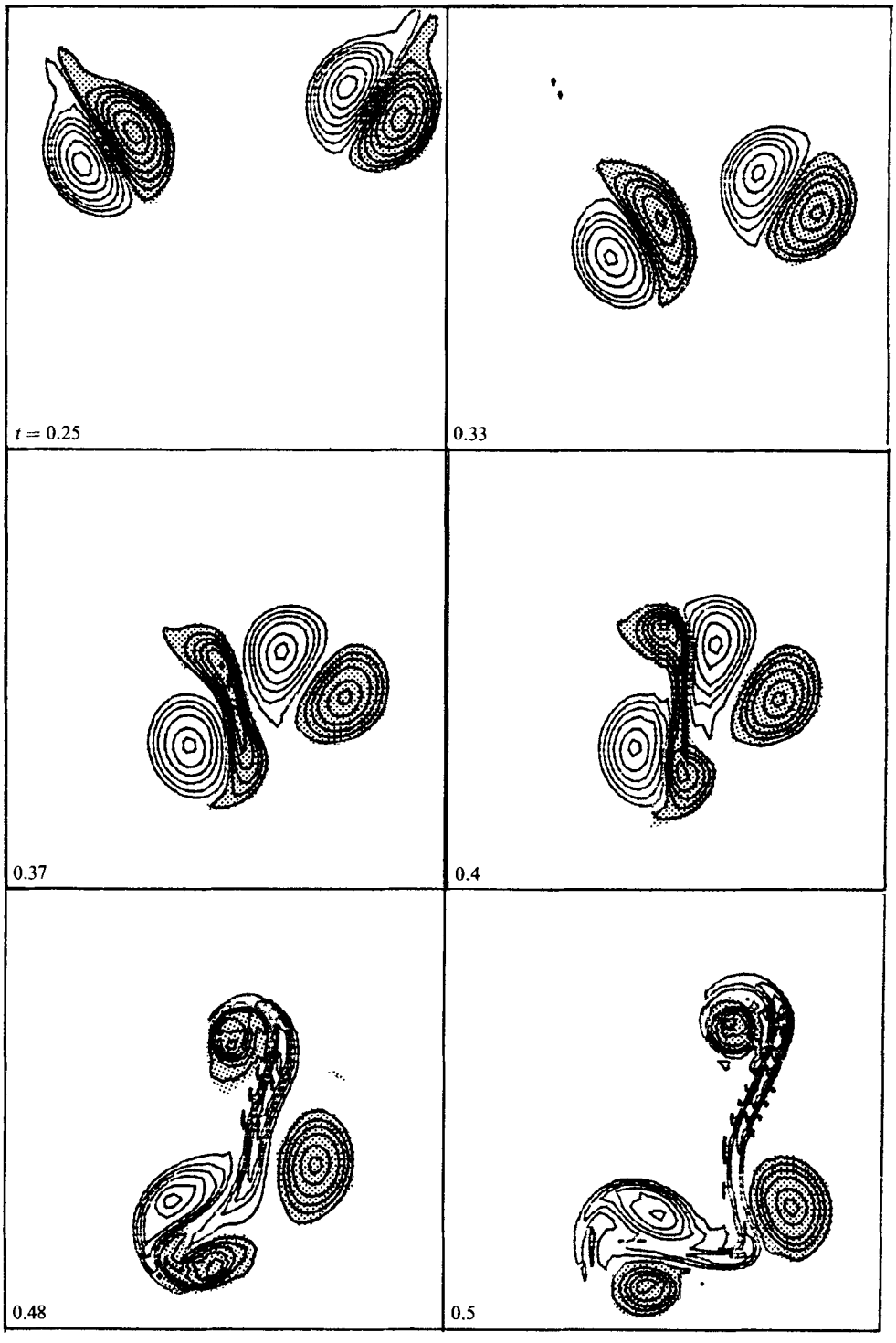

FIGURE 14. Asymmetric lateral collision of two linear couples: vorticity contours at times $t = 0.25$, 0.33, 0.37, 0.4, 0.48 and 0.5. If the collision is inelastic a vortex bursts into two smaller vortices. Shaded areas show positive vorticity.

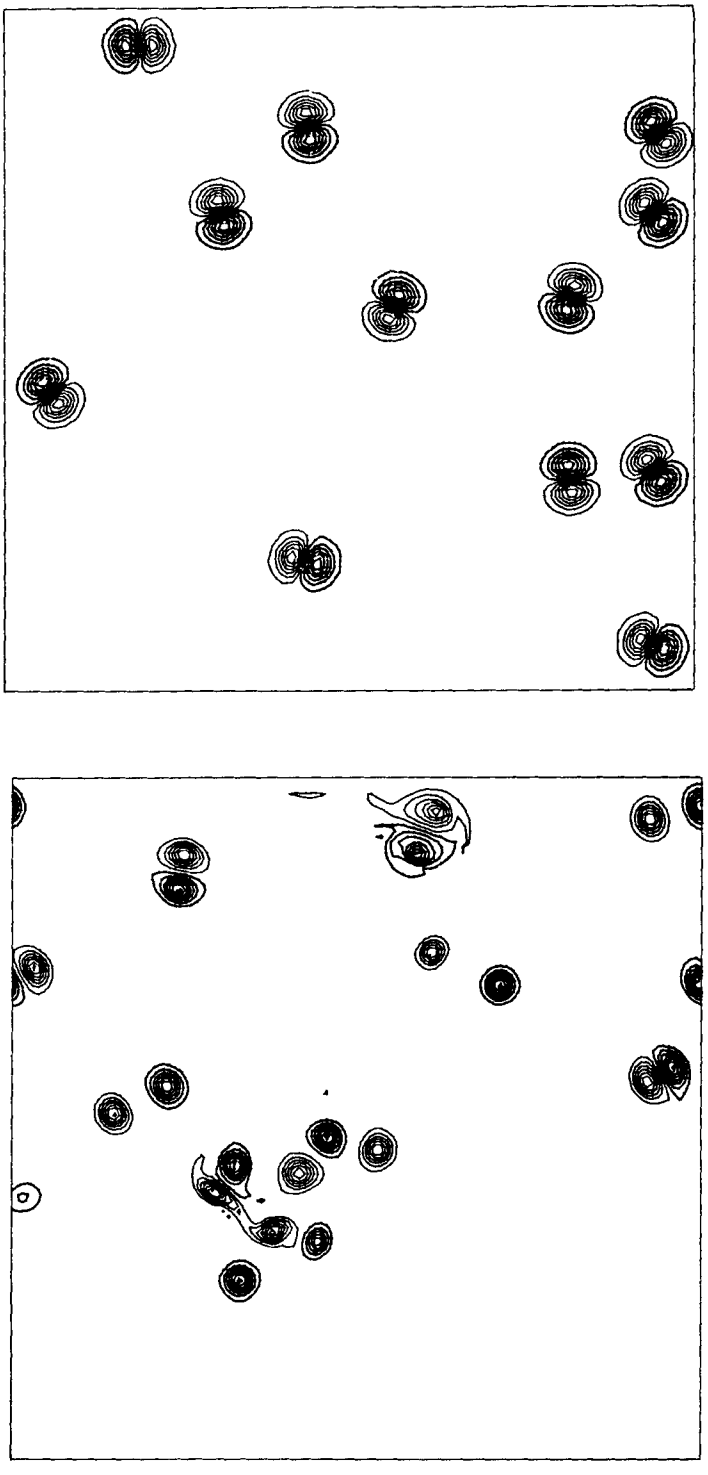

FIGURE 15. A gas of couples (*a*), and its decay into two-dimensional turbulence (*b*).

and its width increases typically as the size of its vortices. A few couples, with a straight trajectory, escape solitarily and move far away until viscosity finally dissipates them. In the absence of visualization a local measurement in the quiescent fluid will detect these couples as sudden bursts of passing vorticity.†

When the number of couples is large (in the turbulent wake of vibrating cylinders for instance) a cloud of couples surrounds the central part of the wake. These couples undergo collisions, most of them destructive, but in spite of their decay their action causes important changes in the wake. They have diffused out the motion and their dissociation leaves a turbulent field of much larger extent than usual. The outer envelope of the disturbed region is formed by a few couples, the fastest, which have escaped interaction.

Gas of couples. In the wakes, isolated vortices, uneven couples and weak structures hasten the decay of couples. This leads to a simpler situation for studying the statistical behaviour of couples. We created a gas of linear couples and investigated its evolution. Owing to the elasticity of certain collisions one could *a priori* think that a number of couples would persist for some time. It is possible both experimentally and numerically to inject a certain density of couples into a region of the plane and to watch their evolution.

Experimentally two disks $d = 3$ mm are towed together side by side at a distance $l = 9$ cm. Both vibrate at the Strouhal frequency. As the velocity is large the wakes are turbulent and generate couples moving in various directions. We study the fluid motion in the centre of the intermediate space. In this region the fluid is at rest except for the couples entering.

In the numerical simulation we initiate a state with identical linear couples randomly distributed in the domain. Figure 15(*a*) shows a typical initial state. The evolution observed experimentally and numerically is the same and shows rapid destruction of the couples. Figure 15(*b*) shows the resulting two-dimensional turbulence. The time of destruction of the couples depends on their initial density. Typically they have been destroyed after having undergone two collisions.

5. Conclusion

The interaction between two vortices depends on whether they are homostrophic or heterostrophic (of the same sign or of opposite sign). We chose to call two vortices of the same sign a pair, and two vortices of opposite sign a couple.

In a pair the vortices orbit around each other and if their distance apart is smaller than a threshold value they roll-up and merge to form a larger vortex. This pairing has been widely studied because in two-dimensional turbulence it is responsible for the reverse energy cascade building up large structures.

In a couple both vortices move together in a translating motion. Among the couples the fastest have a particular structure with a circular envelope and a linear relation between the stream function and vorticity. We have shown that such couples result from initial quadrupolar interaction. Owing to their translation, the role of couples in turbulent flow is to transport energy from one area to another. If the turbulent

† It is worth noting that such bursts also exist in the vicinity of turbulent three-dimensional wakes. Correlation measurements (Townsend 1970) suggest that they are associated with the intermittent passage of couples of vortices. However in the three-dimensional case their axis is oriented differently relative to the wake. A possible interpretation is that coupling of the vortices in the wake took place only in a limited part of their length so that the vortices only moved in this region and formed a loop protruding out of the wake and distorted by the mean flow.

zone is initially limited in space, the couples created near the boundary will have the possibility of escaping. Some of them will undergo collision and decay into turbulence and some will move far away. The boundary between the turbulent zone and the quiescent fluid will thus diffuse out and become increasingly complex, with a few isolated couples intermittently moving across the quiescent fluid.

Inside the turbulent field, couples may be formed locally. They will be very short lived but again they will transport energy. Any zone with less-intense turbulence will allow couples to propagate more easily so that the couples will tend to maintain the homogeneity of the turbulence.

We are very grateful to H. Thomé who designed the experimental set-up. Part of the numerical experiments has been conducted by H. Fabre, B. Laviron, N. Mercier and J. M. Gérard during periods of instruction of the Ecole Polytechnique. We are also indebted to R. M. Philippe, X. Carton, C. Guthmann who helped us at various stages of this work.

REFERENCES

AREF, H. & SIGGIA, E. D. 1981 *J. Fluid Mech.*, **109**, 435–463.

BABIANO, A., BASDEVANT, C., LEGRAS, B. & SADOURNY, R. 1985 *C.R. Acad. Sci. Paris* **229**, 601–604.

BATCHELOR, G. K. 1967 *An Introduction to Fluid Dynamics*, p. 535. Cambridge University Press.

BATCHELOR, G. K. 1969 *Phys. Fluids Suppl.* II **12**, 233–239.

BASDEVANT, C., COUDER, Y. & SADOURNY, R. 1984 In *Macroscopic Modelling of Turbulent Flows*. Lecture Notes in Physics, vol. 230, Springer.

BASDEVANT, C., LEGRAS, B., SADOURNY, R. & BÉLAND, M. 1981 *J. Atmos. Sci.* **38**, 2306–2326.

BASDEVANT, C. & SADOURNY, R. 1983 In *Two Dimensional Turbulence. J. Méc. (numéro spécial)*, p. 243.

BRACHET, M. E. 1986 *Phys. Rev. Lett.* **57**, 683–686.

CHOPRA, K. P. & HUBERT, L. F. 1964 *J. Atmos. Sci.* **22**, 652–657.

COUDER, Y. 1984 *J. Phys. Lett.* **45**, 353–360.

COUDER, Y., BASDEVANT, C. & THOMÉ, H. 1984 *C.R. Acad. Sci. Paris* **299**, 89–94.

DEEM, G. S. & ZABUSKY, N. J. 1978 In *Solitons in Action* (ed. Lonngren & Scott), p. 277–296. Academic.

FORNBERG, B. 1977 *J. Comput. Phys.* **25**, 1–31.

FLIERL, G., LARICHEV, V., MCWILLIAMS, J. & REZNIK, G. 1980 *Dyn. Atmos. Oceans* **5**, 1–41.

GRIFFIN, O. M. & RAMBERG, S. E. 1976 *J. Fluid Mech.* **75**, 257–271.

HOPFINGER, E. J., BROWAND, F. K. & GAGNE, Y. 1982 *J. Fluid Mech.* **125**, 505–534.

KRAICHNAN, R. H. 1967 *Phys. Fluids* **10**, 1417–1423.

KRAICHNAN, R. H. & MONTGOMERY, D. 1980 *Rep. Prog. Phys.* **43**, 547–619.

LAMB, H. 1916 *Hydrodynamics*, 4th edn., pp. 236–237. Cambridge University Press.

LARICHEV, V. & REZNIK, G. 1976 *Rep. Acad. Sci. USSR* **231**, 1077–1079.

LEITH, C. E. 1968 *Phys. Fluids* **10**, 1417–1423.

MCWILLIAMS, J. C. 1983 *Geophys. Astrophys. Fluid Dyn.* **24**, 1–22.

MCWILLIAMS, J. C. 1984 *J. Fluid Mech.* **146**, 21–43.

MCWILLIAMS, J. C., FLIERL, G. R., LARICHEV, V. D. & REZNIK, G. F. M. 1981 *Dyn. Atmos. Oceans* **5**, 219–238.

MCWILLIAMS, J. C. & ZABUSKY, N. J. 1982 *Geophys. Astrophys. Fluid Dyn.* **19**, 207–227.

MEIRON, D. I., SAFFMAN, P. G. & SCHATZMAN, J. C. 1984 *J. Fluid Mech.* **147**, 187–212.

MYSELS, K. J., SHINODA, K. & FRANKEL, S. 1959 *Soap Films, Studies of Their Thinning*. Pergamon.

PIERREHUMBERT, R. T. 1980 *J. Fluid Mech.* **99**, 129–144.

ROSE, H. A. & SULEM, P. L. 1978 *J. Phys. Paris* **39**, 441–484.

ROSHKO, A. 1954 *NACA Tech. Note* 1191.

SAFFMAN, P. G. & SCHATZMAN, J. C. 1982 *J. Fluid Mech.* **117**, 171–185.

SOMMERIA, J. 1983 *J. Méc. Suppl.* 169.

STERN, M. E. 1975 *J. Mar. Res.* **33**, 1–13.

TANEDA, S. 1959 *J. Phys. Soc. Japan* **14**, 843–848.

TAYLOR, G. I. 1959 *Proc. R. Soc. Lond.* A **253**, 296.

THOMSON, W. 1867 *Phil. Mag.* **34**, 20.

TOWNSEND, A. A. 1970 *J. Fluid Mech.* **41**, 13–46.

TSINOBER, A. B. 1975 *Maguitnaya Gidrodinamika, no.* 1, pp. 7–22.

VRIJ, A., HESSELINK, F. TH., LUCASSEN, J. & VAN DEN TEMPEL, M. 1970 *Proc. K. Ned. Akad. Wetensch.* B 73, 124–135.

ZIMMERMAN, L. I. 1969 *J. Appl. Met.* **8**, 896–907.